

Dispersion of the Nonlinear Second-Order Optical Susceptibility of an Organic System: *p*-Nitroaniline

C. C. Teng and A. F. Garito

Department of Physics and Laboratory for Research on the Structure of Matter, University of Pennsylvania, Philadelphia, Pennsylvania 19104

(Received 11 November 1982)

Measurements of the frequency dependence of the microscopic second-order nonlinear electronic susceptibility are reported for the organic system *p*-nitroaniline. The results are suitably described in terms of a theoretical microscopic mechanism involving highly charge-correlated electron states dominating the second-order nonlinear optical response of the system as presented in earlier theoretical calculations.

PACS numbers: 42.65.Cq, 78.20.Dj

Recently, theoretical and experimental interest has centered on the nature of highly charge-correlated π -electron states in organic and polymeric crystalline structures that comprise the microscopic origin of exceptional second-order nonlinear optical responses $\chi_{ijk}^{(2)}(-\omega_3; \omega_1, \omega_2)$, particularly as exhibited in second-harmonic generation (SHG) and linear electro-optic effect (LEO) properties. In one example, 2-methyl 4-nitroaniline crystals possess SHG and LEO figures of merit 50 times those of potassium dihydrogen phosphate that are primarily purely electronic at dc and optical frequencies.¹⁻³ Currently these electronic excitations are viewed as occurring on sites coupled weakly to their neighbors and providing microscopic sources of nonlinear optical response

through the on-site microscopic second-order nonlinear electronic susceptibility β_{ijk} . In the rigid-lattice-gas approximation, $\chi_{ijk}^{(2)}(-\omega_3; \omega_1, \omega_2) = N f^{\omega_1} f^{\omega_2} f^{\omega_3} \beta_{ijk}(-\omega_3; \omega_1, \omega_2)$, where N is the number of sites per unit volume and f^{ω_i} represents local-field corrections.

Lalama and Garito⁴ have presented a detailed theoretical analysis of β_{ijk} and the charge-correlated electron states in the fundamentally important case of *p*-nitroaniline (PNA) (Fig. 1). In second-order perturbation theory with the perturbing Hamiltonian $H' = e \vec{E} \cdot \vec{r} \sin \omega t$, and both the fundamental and created combined frequencies below electronic resonances but well above vibrational and rotational modes, β_{ijk} can be expressed as

$$\beta_{ijk} + \beta_{ikj} = -\frac{e^3}{4\hbar^2} \left[\sum_{\substack{n \neq n' \\ n' \neq g}} (\gamma_{gn}^j \gamma_{n'n}^i \gamma_{gn}^k + \gamma_{gn'}^k \gamma_{n'n}^i \gamma_{gn}^j) \left(\frac{1}{(\omega_{n'g} - \omega)(\omega_{ng} + \omega)} + \frac{1}{(\omega_{n'g} + \omega)(\omega_{ng} - \omega)} \right) \right. \\ + (\gamma_{gn}^i \gamma_{n'n}^j \gamma_{gn}^k + \gamma_{gn'}^i \gamma_{n'n}^k \gamma_{gn}^j) \left(\frac{1}{(\omega_{n'g} + 2\omega)(\omega_{ng} + \omega)} + \frac{1}{(\omega_{n'g} - 2\omega)(\omega_{ng} - \omega)} \right) \\ + (\gamma_{gn}^j \gamma_{n'n}^k \gamma_{gn}^i + \gamma_{gn'}^k \gamma_{n'n}^j \gamma_{gn}^i) \left(\frac{1}{(\omega_{n'g} - \omega)(\omega_{ng} - 2\omega)} + \frac{1}{(\omega_{n'g} + \omega)(\omega_{ng} + 2\omega)} \right) \\ \left. + 4 \sum_n [\gamma_{gn}^j \gamma_{gn}^k \Delta r_n^i (\omega_{ng}^2 - 4\omega^2) + \gamma_{gn}^i (\gamma_{gn}^k \Delta r_n^j + \gamma_{gn}^j \Delta r_n^k) (\omega_{ng}^2 + 2\omega^2)] \right. \\ \left. \times \frac{1}{(\omega_{ng}^2 - \omega^2)(\omega_{ng}^2 - 4\omega^2)} \right], \quad (1)$$

where summations are over complete sets of eigenstates $|n\rangle$ and $|n'\rangle$ of the unperturbed system, $\gamma_{n'n}^i = \langle n | r^i | n' \rangle$, $\Delta r_n^i = r_{nn}^i - r_{gg}^i$, and $\hbar\omega_{ng}$ is the difference between excited and ground-state energies.

A configuration-interaction calculation with the PNA singlet excited states (4.2, 4.37, 4.38, 5.57, 6.17, 6.63, 6.80, 7.06, and 7.49 eV) showed that the dominant contribution to the measured β_{ijk} value is contained in the last summation term,

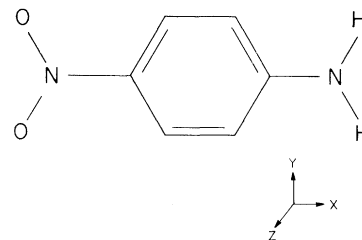


FIG. 1. Molecular structure of PNA.

TABLE I. Comparison of experimental and theoretical β_x values of PNA. β_x^{exp} is the experimental value; β_x^d , the calculated value accounting for solvent effect; and β_x^g , the gas-phase calculated value from Ref. 4.

λ (μm)	$\hbar\omega$ (eV)	β_x^{exp} (10^{-30} esu)	β_x^d (10^{-30} esu)	β_x^g (10^{-30} esu)
1.907	0.650	9.6 ± 0.5	9.5	5.7
1.370	0.905	11.8 ± 0.3	11.6	6.4
1.060	1.170	16.9 ± 0.4	15.9	7.7
0.909	1.364	25 ± 1.0	24	9.2
0.830	1.494	40 ± 3.0	35	10.7

especially the virtual excitations to the highly correlated second excited state ($\hbar\omega_{ng} = 4.37$ eV).⁴ This latter result provided a firm basis for convenient quasi one-dimensional two level phenomenological models for organic structures.^{5,6}

In this paper we report the first measurements of the frequency dependence (dispersion) of β_x , the vector part of β_{ijk} , for an organic system by having performed dc-induced second-harmonic generation measurements on liquid dioxane solutions of PNA. The results provide a direct test of current theoretical descriptions and understanding of second-order nonlinear optical processes occurring in these novel structures. In the experiment, a tunable pulsed dye laser (Quanta Ray) was used as a pump beam into a compressed H₂ gas cell, generating Stokes lines from stimulated Raman scattering tunable from 0.2 to 2 μm . The dc-induced second-harmonic generation experiment was performed by the wedge cell technique with synchronous dc voltage pulses as described earlier.⁷ The measurements utilized several different fundamental wavelengths of incident power well below solution damage thresholds and were referenced to d_{11} of quartz (1.2×10^{-9} esu).⁸

In the infinite-dilution limit, solute-solute and solvent-solvent interactions were minimized with Onsager local-field corrections.⁷ In the C_{2v} symmetry for PNA and second-harmonic generation, β_x is given by

$$\beta_x = \beta_{xxx} + \frac{1}{3}[\beta_{xyy} + \beta_{xzz} + 2\beta_{yyx} + 2\beta_{zzx}],$$

where the x direction is along the molecular dipole axis (Fig. 1).

The frequency-dependent experimental values (β_x^{exp}) of β_x for PNA are listed in Table I and plotted in Fig. 2. As the fundamental frequency is increased, β_x^{exp} rapidly increases smoothly as 2ω approaches the excitation frequency ($\omega_{ng} \sim 3.5$ eV/ \hbar) which is the first major optical-absorption peak of PNA in dioxane corresponding

to excitations to the important second excited state.

The difference between the experimental β_x^{exp} values and calculated gas-phase β_x^g results of PNA (Table I) is due to well-known solvent-induced shifts of the singlet-singlet excitation energies easily observable in solution absorption spectra.⁹ The PNA permanent dipole moment (μ) polarizes the surrounding nonpolar dioxane solvent medium, causing an induced dipole moment proportional to μ with an interaction energy $E = A\mu^2$, where $A = -a^{-3}f(n)$, a is the cavity radius containing the PNA, and $f(n)$ is a standard function of the refractive index of the solvent medium.⁹ The shift in the excitation energy ($\hbar\omega_{ng}$) is caused by changes in the difference between the PNA ground- and excited-state dipole moments which in turn is an important quantity determining the magnitude of β_x :

$$\Delta\omega_{ng} = (A/\hbar)(\mu_n^2 - \mu_g^2),$$

where $\mu_i = -er_{ii}^x$. The measured shifts in the

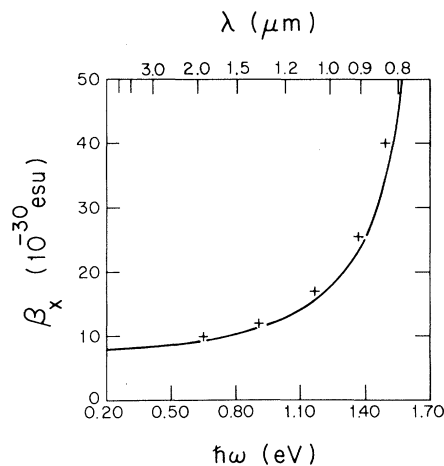


FIG. 2. Frequency dependence of β_x for PNA: (pluses) experimental β_x^{exp} data points, and (solid line) theoretical β_x^d curve accounting for solvent effect.

singlet-singlet excitation spectrum of PNA in dioxane provide a new set of state energies (4.41, 3.51, 4.2, 4.86, 5.58, 6.53, 7.01, 6.63, and 7.63 eV). These energies were used in Eq. (1), yielding the β_x^d values listed in Table I and the calculated dispersion curve (solid line) shown in Fig. 2. Within experimental error, the agreement between experiment and theory is quite satisfactory. Further refinement such as accounting for minor solvent-induced changes in the matrix elements of Eq. (1) would result in an even closer agreement by 10%–15% increase in the calculated β_x values.

In summary, measurements of the dispersion of β_x for PNA have demonstrated that the theoretical microscopic mechanism is essentially correct in describing the second-order nonlinear optical response in terms of highly charge-correlated electron states. Importantly, the effect of solvent enhancement on β_x is adequately understood in terms of a solute-solvent reaction field mediated by dipole-dipole interactions. Recently completed studies of β_{ijk} on related systems and detailed experimental descriptions will be reported separately.

This research was supported by the National Science Foundation Materials Research Laboratory program under Grant No. DMR-7923647 and by

the Defense Advanced Research Projects Agency under Grant No. DAAK-70-77-C-0045 (5-26502). We gratefully thank Dr. K. D. Singer, C. Grossman, and Dr. O. Zamani-Khamiri for many helpful discussions and Dr. A. McGhie for help in sample preparation.

¹B. F. Levine, C. G. Bethea, C. D. Thurmond, R. T. Lynch, and J. L. Bernstein, *J. Appl. Phys.* **50**, 2523 (1979).

²G. F. Lipscomb, A. F. Garito, and R. S. Narang, *J. Chem. Phys.* **75**, 1509 (1981).

³A. F. Garito and K. D. Singer, *Laser Focus* **18**, 59 (1982).

⁴S. J. Lalama and A. F. Garito, *Phys. Rev. A* **20**, 1179 (1979).

⁵B. F. Levine, *Chem. Phys. Lett.* **37**, 516 (1976).

⁶J. L. Oudar and J. Zyss, *Phys. Rev. A* **26**, 2016 (1982).

⁷K. D. Singer and A. F. Garito, *J. Chem. Phys.* **75**, 3572 (1981).

⁸M. Choy and R. L. Byer, *Phys. Rev. B* **14**, 1693 (1976). The variation of d_{11} over the working frequency range is only a few percent according to Miller's rule.

⁹See, for example, A. T. Amos and B. L. Burrows, *Adv. Quantum Chem.* **7**, 289 (1973), and references therein.